



Deoxy-sugar releasing biodegradable hydrogels promote angiogenesis and stimulate wound healing

Muhammad Yar^{a,*}, Lubna Shahzadi^a, Azra Mehmood^b, Muhammad Imran Raheem^a, Sabiniano Román^c, Aqif Anwar Chaudhry^a, Ihtesham ur Rehman^a, C.W. Ian Douglas^d, Sheila MacNeil^{c,*}

^a Interdisciplinary Research Center in Biomedical Materials (IRCBM), COMSATS Institute of Information Technology, Lahore, 54000, Pakistan

^b Center of Excellence in Molecular Biology (CEMB), Lahore, 54000, Pakistan

^c The Kroto Research Institute, Materials Science and Engineering, North Campus, University of Sheffield, Broad Lane, Sheffield, S3 7HQ, UK

^d Unit of Oral and Maxillofacial Pathology, School of Clinical Dentistry, University of Sheffield, Clarendon Crescent, Sheffield, South Yorkshire, S10 2TA, United Kingdom

ARTICLE INFO

Keywords:

Angiogenesis
Sugars
Hydrogels
Chitosan

ABSTRACT

Vascular endothelial growth factor (VEGF) stimulates endothelial cells to migrate, proliferate and form new blood vessels. However direct delivery of VEGF has not become clinically adopted as a means of stimulating blood vessel formation and wound healing because of its relatively poor stability and its production of immature blood vessels. A simpler way of stimulating production of VEGF *in situ* is explored in this study following reports of deoxy sugars involved in inducing VEGF production. The pro-angiogenic effect of L and D isomers of deoxy sugars (ribose, fucose and rhamnose) loaded into biodegradable chitosan/collagen hydrogels was examined using a chick chorioallantoic membrane assay. The L-sugars were all pro-angiogenic but only the 2-deoxy-D-ribose had strong effects on angiogenesis. Furthermore, these sugars could not be metabolised by four strains of *Staphylococcus aureus*, as a metabolic substrate for growth, although some of these could be metabolised by another typical pathogen, *Pseudomonas aeruginosa*. The effects of 2-deoxy-D-ribose in a chitosan/collagen hydrogel on wound healing were also assessed. This biomaterial doubled the rate of cutaneous wound healing in rats associated with an increase in vascularisation detected by staining for CD34 positive cells.

1. Introduction

Angiogenesis is a key issue in wound healing. Of all the angiogenic factors, the most potent one and commonly used is vascular endothelial growth factor (VEGF) [1–4]. This growth factor can be produced by recombinant technology and it has been examined critically in many studies [5–7]. However, results have been generally disappointing when it is added on its own as it is rapidly broken down or diluted and washed away. Recent strategies have considered developing VEGF bound to biomaterials including hydrogels, electrospun scaffolds or particles [8–11].

Heparin is a natural glycosaminoglycan present in the body at high concentrations in wounds where it acts to bind VEGF and other pro-angiogenic factors [12,13]. The MacNeil group have developed materials where they have sought to immobilise heparin on an electrostatic basis either to hydrogels [14] or in a layer by layer coating of electrospun scaffolds [13,15]. *In vivo* heparin binds and releases VEGF and other pro-angiogenic mitogens [16]. VEGF activates the proliferation

and migration of endothelial cells in both normal and tumour tissue and results in rapid generation of new blood vessels [17,18]. Accordingly VEGF's potential has been explored in the preparation of materials where angiogenesis is required, for example in the preparation of synthetic dermis for the treatment of full thickness burns injuries [19–21] and to stimulate wound healing in chronic non-healing wounds such as diabetic ulcers where the microvasculature is compromised. The need for both is discussed later in this manuscript.

Although VEGF stimulates angiogenesis it is very expensive (930\$ for 50 µg from Sigma-Aldrich), and is not stable [22,23]. Also, VEGF is not the only pro-angiogenic growth factor involved in new blood vessel formation and, *in vivo*, it is normally produced as part of a coordinated wound healing programme with a complex cascade of factors that are produced and released in response to hypoxia.

In contrast to the normally well-regulated production of new blood vessels, in tumours vasculogenesis is exaggerated. A recent study (Yar et al., 2014) showed that one of the enzymes that is highly active in producing excessive vasculature in tumours, phosphorylase kinase,

* Corresponding authors.

E-mail addresses: dmyar@ciitlahore.edu.pk (M. Yar), s.macneil@sheffield.ac.uk (S. MacNeil).

leads to the production of 2-deoxy-D-ribose. This D-sugar in turn leads to the production of VEGF in tumourigenesis [24].

As 2-deoxy-D-ribose supports angiogenesis under these circumstances, we hypothesised that the gradual release of this sugar will promote new blood vessels formation via the production of VEGF. In addition, this molecule is stable and inexpensive and can be introduced into biomaterials to hopefully give sustained release over several days to stimulate the growth of new blood vessels.

To test this hypothesis L and D-isomers of deoxy-sugars were loaded into biodegradable chitosan (CS)/collagen freeze gelled hydrogels which were examined for their ability to support the formation of new blood vessels using the chick chorionic allantoic membrane (CAM) assay. It is important, however, to avoid promoting infection by providing simple bacterial growth substrates in biomaterials and although it is reported that many bacteria cannot metabolise 2-deoxy-D-ribose [25], we examined whether the L and D-isomers of deoxy-sugars could be fermented by typical soft tissue pathogens. Finally, we examined the ability of a CS/collagen hydrogel containing 2-deoxy-D-ribose to accelerate wound healing in a rat skin wound model.

2. Experimental section

2.1. Materials

L-rhamnose and NaOH were purchased from Sigma-Aldrich (USA). CS was purchased from Mian Scientific Company, Lahore, Pakistan and further purified in our laboratories (degree of deacetylation (DD) 84%; Mw: 87047.26 g/mol) [26]. Collagen was purchased from Mian Scientific suppliers Lahore. PVA (Mw: 72,000, degree of hydrolysis 98%), hydrochloric acid (HCl) was purchased from Merck (Germany). Triethyl orthoformate (98%) was purchased from Alfa Aesar (Germany). Glacial acetic acid (CH_3COOH) was purchased from AnalaR BDH Laboratory Supplies (UK). Ethanol (99.8%) was purchased from Sigma-Aldrich (Germany.) 2-deoxy-D-ribose, D-fucose and L-fucose were purchased from Sigma-Aldrich China, UK and Slovakia, respectively. 2-deoxy-L-ribose and D-rhamnose were products of Carbosynth (UK). Brain Heart Infusion broth and Tryptone soy broth (1% w/v) were purchased from Oxoid Ltd. Phenol red was purchased from Sigma-Aldrich UK.

2.2. Preparation of cross-linked chitosan/collagen hydrogels by freeze gelation

CS and collagen (0.5 g each) were dissolved in acetic acid (0.5 M, 20 mL) and stirred at room temperature until completely dissolved and a clear solution was obtained. To this, triethyl orthoformate (4% v/v, 0.8 mL) was added as a cross-linker and the solution was further stirred overnight for better homogeneity and cross-linking of materials. The mixture was then poured into a petri dish and frozen at $-20\text{ }^\circ\text{C}$ overnight. The frozen membranes were then immersed in pre-cooled ethanolic sodium hydroxide (3N) and again placed at $-20\text{ }^\circ\text{C}$ for 24 h. After that, the frozen membranes were washed in 50% (v/v) ethanol solution and then with distilled water to remove the sodium hydroxide. The membranes were finally washed twice in absolute ethanol for 15 min and dried at room temperature to obtain porous hydrogels.

2.3. Deoxy-sugar loading of hydrogels

For sugar loading, hydrogels were soaked in a 1 mg/ml aqueous solution for the 2 isoforms (D and L) of the 3 sugars (ribose, fucose and rhamnose) at $37\text{ }^\circ\text{C}$ until all the liquid had been absorbed by the hydrogels (6 groups in total). Following storage at $-20\text{ }^\circ\text{C}$ overnight, hydrogels were dried in a lyophilizer (Christ, Alpha 1–2 LD plus, Germany) at $-40\text{ }^\circ\text{C}$ before further characterization.

2.4. Fourier transform infrared spectroscopy analysis

The infrared (FT-IR) spectra were recorded on photo acoustic mode at the frequency range of $4000\text{--}400\text{ cm}^{-1}$ with 256 consecutive scans at 8 cm^{-1} resolution on a Thermo-Nicolet 6700 P Fourier transform infrared spectroscopy (FTIR) Spectrometer (USA).

2.5. Scanning electron microscopy

The surface morphology of the composite matrices was examined under scanning electron microscope (SEM), Model JEOL JSM 6480. The samples were gold sputtered coated prior to examination at a range of magnifications.

2.6. Assessment of angiogenic properties of hydrogels using the chick chorionic allantoic membrane assay

Fertilized chicken (*Gallus domesticus*) eggs were purchased from Big Bird (Raiwind road, Lahore, Pakistan) and incubated at $37\text{ }^\circ\text{C}$ from day 2 of fertilization until day 8 in a humidified egg incubator (HHD, 435, China). At day 8, a square window (1 cm^2) was cut into the shell and removed, and a 2 cm^2 piece of the hydrogel placed onto the CAM. Each egg was implanted with one hydrogel only (L and D isoforms of 3 deoxy-sugars).

The shell window was closed with parafilm (Bemis Flexible Packaging, USA) and sealed with adhesive tape. After implantation, eggs were placed again at $37\text{ }^\circ\text{C}$ in a 40% humidified incubator until day 14. At day 14, biomaterials were retrieved and the eggs were sacrificed. Angiogenesis was quantified by taking light microscope pictures just before biomaterials were retrieved and then blindly scored by four assessors using images. The number of implanted and survived eggs is given in the caption of respective CAM assay figures.

2.7. Fermentation of sugars by bacteria

The six sugars under investigation were compared to glucose with respect to acting as substrates for metabolism by representative common pathogens in wound infections.

2.7.1. Bacteria

Five bacterial strains were employed in the study; four strains of *Staphylococcus aureus* and one strain of *Pseudomonas aeruginosa*. The *S. aureus* strains were S235 – a recent clinical isolate that was used in development of a bacterial infected skin model reported from this laboratory previously [27]. NCTC 6571 (Oxford) – a reference strain commonly used as a for antibiotic sensitivity testing; strain Newman – originating from a clinical infection but which has a defect in surface fibronectin binding protein, and L-9879 – another clinical isolate but which is hydrophilic.

2.7.2. Growth and fermentation of sugars

Bacteria were grown in Brain Heart Infusion broth for 16 h at $37\text{ }^\circ\text{C}$. Aliquots (100 mL) of Tryptone Soy broth (1% w/v) supplemented with phenol red (0.02% w/v; Sigma-Aldrich UK) and appropriate sugars (1% w/v final conc.) were added to sterile 96 well plates. 5 mL of the overnight broth cultures of each bacterial strain was then added to wells and incubated for 16 h at $37\text{ }^\circ\text{C}$. The ability of each strain to ferment each sugar was judged by the production of acid and change of the phenol red pH indicator.

2.8. Full-thickness excisional rat wound model

For *in vivo* experiments, only the 2-deoxy-D-ribose freeze gelled hydrogels were tested. 20 mm diameter and 1.2 mm thickness circles were prepared. The samples were sterilized using ethanol (70%) solution, air dried and equilibrated in PBS briefly before placing on the

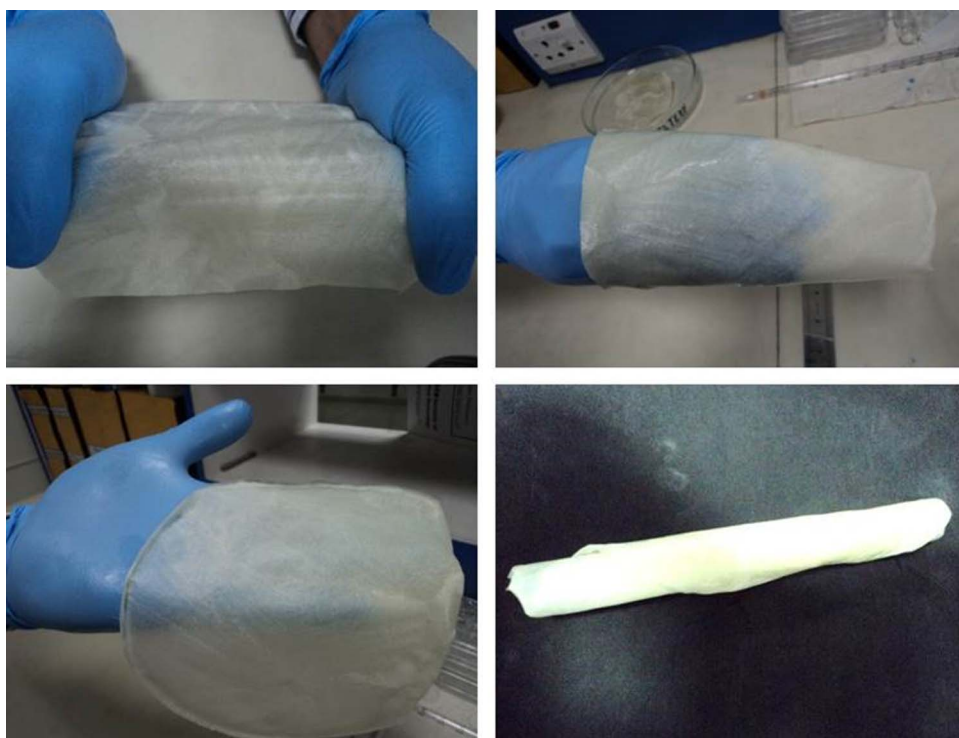


Fig. 1. Photographs of chitosan (CS)/collagen hydrogels to show their shape, flexibility, and ability to be folded.

wound. For animal trials, male Sprague-Dawley (SD) rats weighing 140–170 g were used in the study. The animals had free access to food and water and were kept in a dedicated animal house facility according to procedures approved by the Institutional Animal Ethics Committee at CEMB, Lahore, Pakistan. Animals were anesthetized with ketamine (100 mg/kg body weight) and xylazine (10 mg/kg body weight) and then the fur from the dorsal side was removed with a hair trimmer (Dingling professional hair clipper, RF-608, China). The backs of the rats were completely shaved for adhesive tape fixation and dressing. After shaving, the backs were cleaned with ethanol and then they were transferred onto a clean sterilized table and three circular shaped wounds were created by removing skin at three marked areas with the help of surgical scissors (Noorani Surgical Medical Supplies, Pakistan). Immediately followed the excision process, one of these wounds was covered with sterilized, 2-deoxy-D-ribose –loaded (using 70% ethanol) membrane circles and the other was covered with the same material membranes but without any 2-deoxy-D-ribose. Both implanted membranes were sutured in position using sterile braided silk sutures (Mersilk, diameter 220 μm). The hydrogels were covered with adhesive plaster (Mepore, Sweden), further dressed with cotton gauze and finally secured with white surgical adhesive tape (Nitto, Japan) to prevent damage from self-grooming. Surgical dressings were removed three days after membrane implantation.

A negative control group was included. For this the wound was kept open and covered with dressing only (Mepore, Sweden) which was left to heal naturally (sham operated control). Control hydrogel (without sugar) and hydrogel loaded with D-deoxy-ribose were implanted. For each group, three rats were used and on days 0, 3, 9, 11, 14 and 17 post-wounding, the wounds were photographed. The average diameter of the wound was determined using Image J from four independent calculations for each sample. By the end of experiments, on day 17, rats were euthanized with an overdose of anaesthesia and tissue sections from implantation sites of normal, sham, control (hydrogels without 2-deoxy-D-ribose) and 2-deoxy-D-ribose loaded hydrogels treated groups were removed. The samples were fixed in 3.7% paraformaldehyde (Sigma-Aldrich, USA) solution for 24 h at room temperature. They were dehydrated using various concentrations of ethanol and water from

70% to 100% and paraffin blocks were made.

2.8.1. Histology

Sections of 6 μm thick were cut from the paraffin embedded samples with a microtome (Leica TP 1020 Automatic Tissue Processor) and placed on Superfrost[®] plus slides (Menzel-Gläser, Denmark). Conventional Haematoxylin and Eosin (H & E) staining and Gouldner's trichrome staining was performed, as previously described [28], before mounting in DPX mounting medium (Fisher Scientific) with a coverslip.

For immunohistochemistry (IHC), 6 μm sections were processed with a mouse/rabbit specific HRP/DAB (ABC) Detection IHC Kit (Abcam). After rehydration, antigen retrieval and protein blocking steps, the sections were incubated with 3 different monoclonal antibodies (rabbit anti-CD34 (Abcam) 1:1000, mouse anti-CD80 (Santa Cruz) 1:100 and mouse anti-CD163 (AbD Serotec) 1:300) for 2 h diluted in 1% BSA (Sigma-Aldrich). This was followed by 10 min incubation with a secondary biotinylated goat anti-polyvalent antibody (Abcam Detection IHC Kit). After incubation with an avidin and biotinylated horseradish peroxidase, the target proteins were visualized by incubation in peroxidase substrate and DAB chromogen (Abcam Detection IHC Kit). Samples were then counterstained with haematoxylin, dehydrated, and mounted as per H & E protocol. Controls consisted of samples incubated without primary and secondary antibodies, or incubated only with secondary antibodies. Semi-quantitative assessment of the extent of immunostaining was performed on a blinded observer basis using a qualitative grading scale; absent = 0, mild presence = 1, large presence = 2, abundance = 3, great abundance = 4. Five representative images from each sample at each time point were assessed by two blinded researchers (n = 10). Example photographs depicting 0, 1, 2, 3 and 4 were provided for reference and the median value from these scores was used. The M1/M2 ratio was also calculated for each using the values from the blind scoring of the immunostaining.

2.9. Statistics

Differences between groups for the immunostaining were tested with a non-parametric Kruskal-Wallis test and multiple comparisons

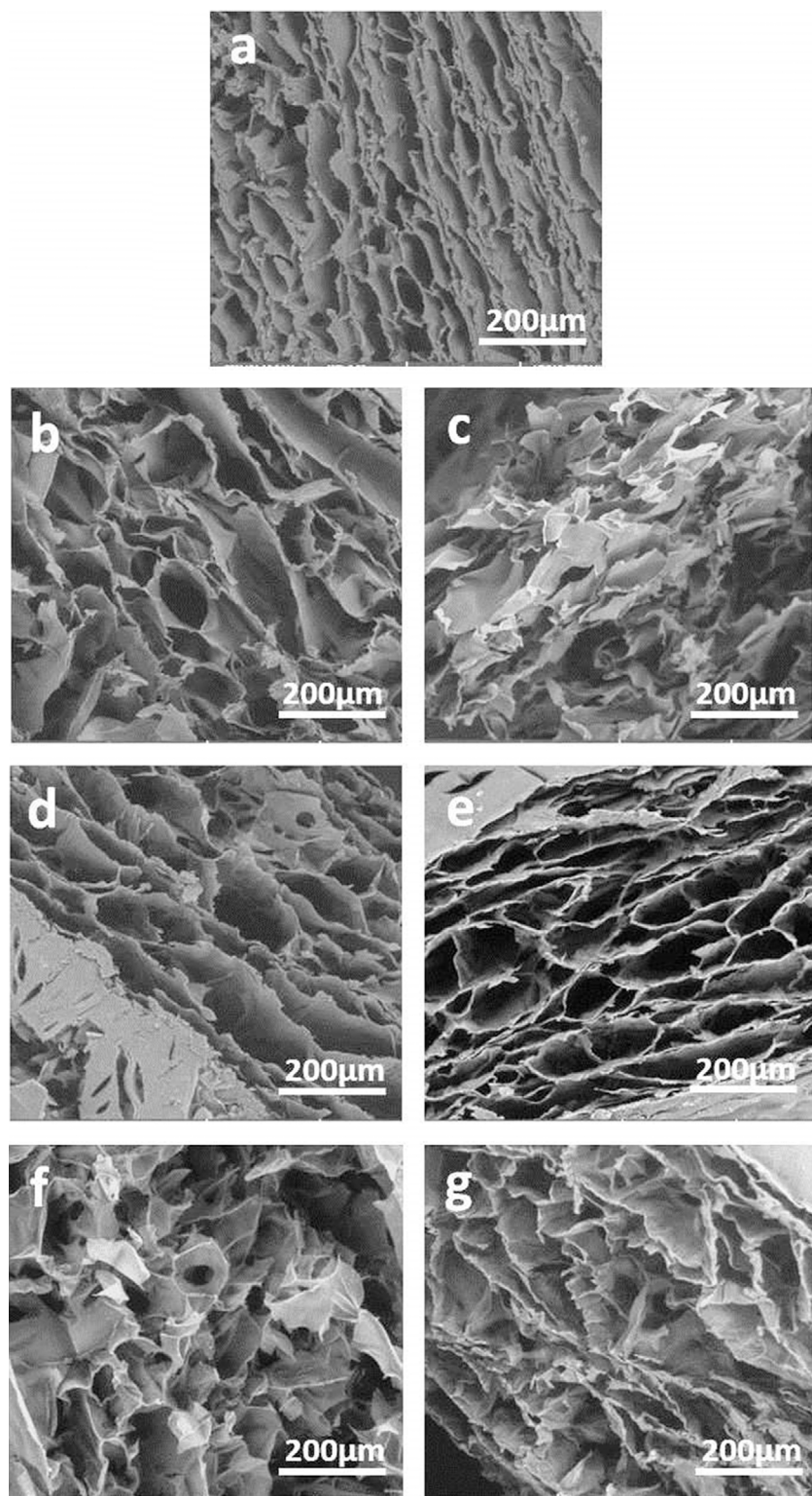


Fig. 2. Scanning Electron Microscope (SEM) micrographs of cross-linked CS/Collagen hydrogel showing cross-sectional view of hydrogels. Micrographs revealing porous structure of the hydrogels, Magnification 200X; (A) control (without sugars), (B) D-deoxy-ribose loaded hydrogel, (C) L-deoxy-ribose loaded hydrogel, (D) D-deoxy-rhamnose loaded hydrogel, (E) L-deoxy-rhamnose loaded hydrogel, (F) D-deoxy-fucose loaded hydrogel, (G) L-deoxy-fucose loaded hydrogel.

between individual groups using a Dunn's test.

3. Results

3.1. Physical appearance of the hydrogel before loading sugars

The average hydrogel thickness, before submersion in saline, was 1.11 mm and after 24 h of submersion it increased to 1.37 mm. The values are the average of three independent experiments. It is critical to

assess the physical stability of the membranes as eventually the materials will be handed over to a surgeon for application to the skin. The surface of the membranes was smooth and devoid of any cracks. Fig. 1 shows the physical appearance of this membrane before and after being stretched, and its ability to be draped for surgical procedures. Moreover, these membranes could be easily cut with a blade or scissors into the desired shape. On handling, the membranes were strong and flexible and could be stretched.

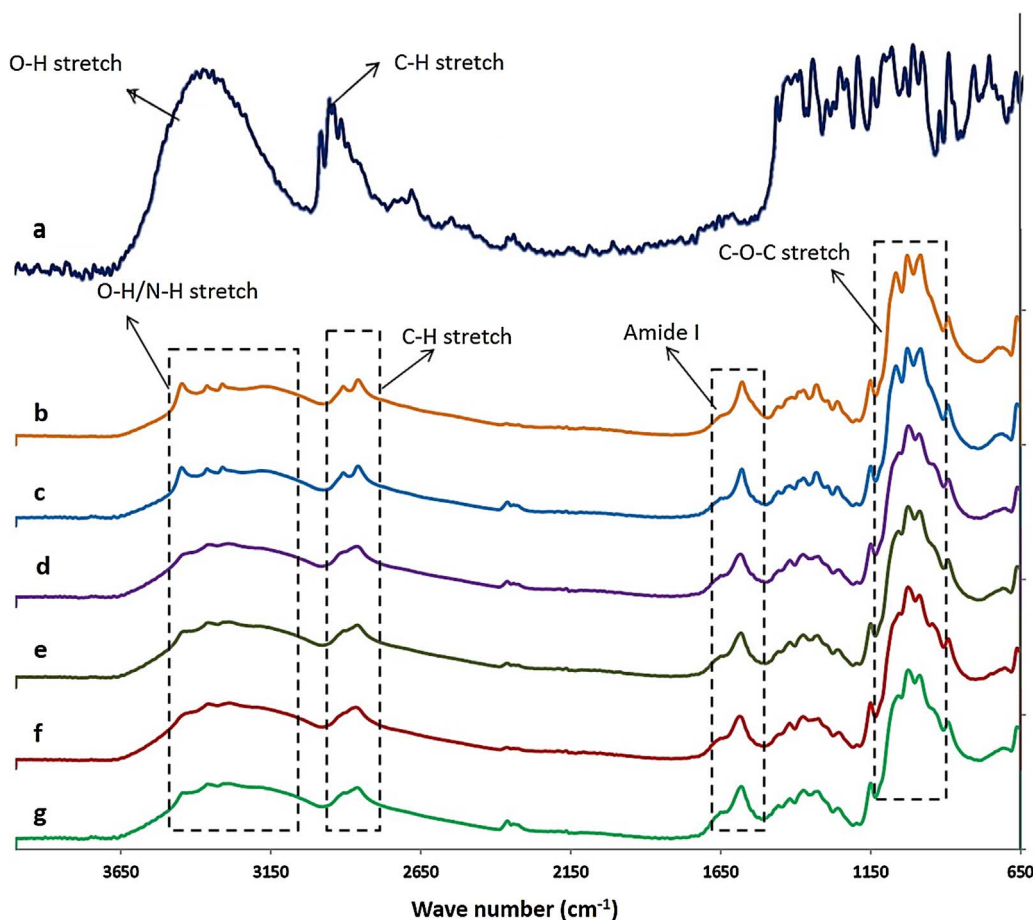


Fig. 3. FTIR spectrum of (a) D-deoxy-ribose; FTIR of CS/Collagen hydrogels (a) D-deoxy-fucose loaded hydrogel, (b) L-deoxy-fucose loaded hydrogel, (c) L-deoxy-rhamnose loaded hydrogel, (d) D-deoxy-rhamnose loaded hydrogel, (e) L-deoxy-ribose loaded hydrogel, (f) D-deoxy-ribose loaded hydrogel, (g) control (without sugars).

3.2. Morphological and chemical characterization of the hydrogel after loading of sugar

3.2.1. Scanning electron microscope

To investigate how different sugars affect the structure and morphology of hydrogels, which plays a critical role in cell infiltration and proliferation, the microscopic structures of these sugar-loaded hydrogels were examined by SEM (Fig. 2). A sheet-like structure with an average pore size of $75.07 \pm 34.48 \mu\text{m}$ was observed in the case of the control hydrogels (Fig. 2a). The average pore-size of hydrogels containing D and L-deoxy-ribose was $100.04 \pm 24.01 \mu\text{m}$ and $93.33 \pm 23.49 \mu\text{m}$, respectively (Fig. 2b and c). In the case of hydrogels containing D and L-deoxy-rhamnose (Fig. 2e), the average pore-size was $102.45 \pm 23.05 \mu\text{m}$ and $110.89 \pm 20.56 \mu\text{m}$, respectively. Hydrogels containing D and L-fucose showed average cross-sectional pore-sizes of $72.18 \pm 16.92 \mu\text{m}$ and $87.43 \pm 14.11 \mu\text{m}$ respectively. Thus, the SEM micrographs demonstrated that all the sugar-loaded hydrogels had similar highly porous structures.

3.2.2. Fourier transform infrared spectroscopy

FTIR spectroscopy was used to look at the interactions between the sugar and the polymers. Fig. 3 shows that the major peak for D-ribose seen at around 3400 cm^{-1} . The peaks of alkyl groups, in D-sugar, showed absorbance peaks between 2700 and 2900 cm^{-1} .

The spectra of hydrogels contain all the characteristic peaks of CS and collagen. The peaks near 2900 cm^{-1} were assigned to C–H stretching vibrations [29]. The bands which appeared near 1400 cm^{-1} were due to C–H bending vibrations. The peaks at 1099 cm^{-1} were due to C–O–C stretching vibrations. However, in the cross-linked hydrogel spectrum, O–H and N–H stretches also appeared at 3400 – 3200 cm^{-1} [30] as a broad peak, but there was significant decrease in the intensity

of this hump. This may be due to the utilization of $-\text{NH}_2$ of CS in forming new $-\text{C}=\text{N}$ bond. The new peak of the imine bond appeared at 1630 cm^{-1} [31,32].

3.3. Assessment of pro-angiogenic responses to deoxy-sugar-loaded biomaterials using the chorionic allantoic membrane assay

As can be seen in Fig. 4 all three of the L isomers stimulated angiogenesis (Fig. 4C, E and G) compared to the control (without sugars). However, for the D isomers, only the D isomer of deoxy-ribose was strongly angiogenic (Fig. 4B). There was no significant response to the D isomer of deoxy-fucose and only a marginal response to the D isomer of deoxy-rhamnose.

3.4. Ability of bacteria to metabolise l and d deoxy-sugars

While all four *S. aureus* strains could use glucose for fermentation, none of these strains were able to use L- or D-isomers of the three deoxy-sugars tested as a substrate. *P. aeruginosa* was, however, able to ferment all sugars except for the L isomers of deoxy-fucose and deoxy-rhamnose (Table 1).

3.5. Assessment of wound healing responses to deoxy-D-ribose loaded freeze gelled hydrogel using a rat cutaneous wound model

Wound healing in rats was accelerated by the application of 2-deoxy-D-ribose-loaded freeze gelled hydrogels. Representative macroscopic pictures of wounds are shown in Fig. 5. Groups including sham operated, control hydrogels (without sugars) and 2-deoxy-D-ribose-loaded hydrogels are shown at days 3, 9, 11, 14 and 17 post-wounding.

In conducting the animal experiments the initial hydrogel was quite

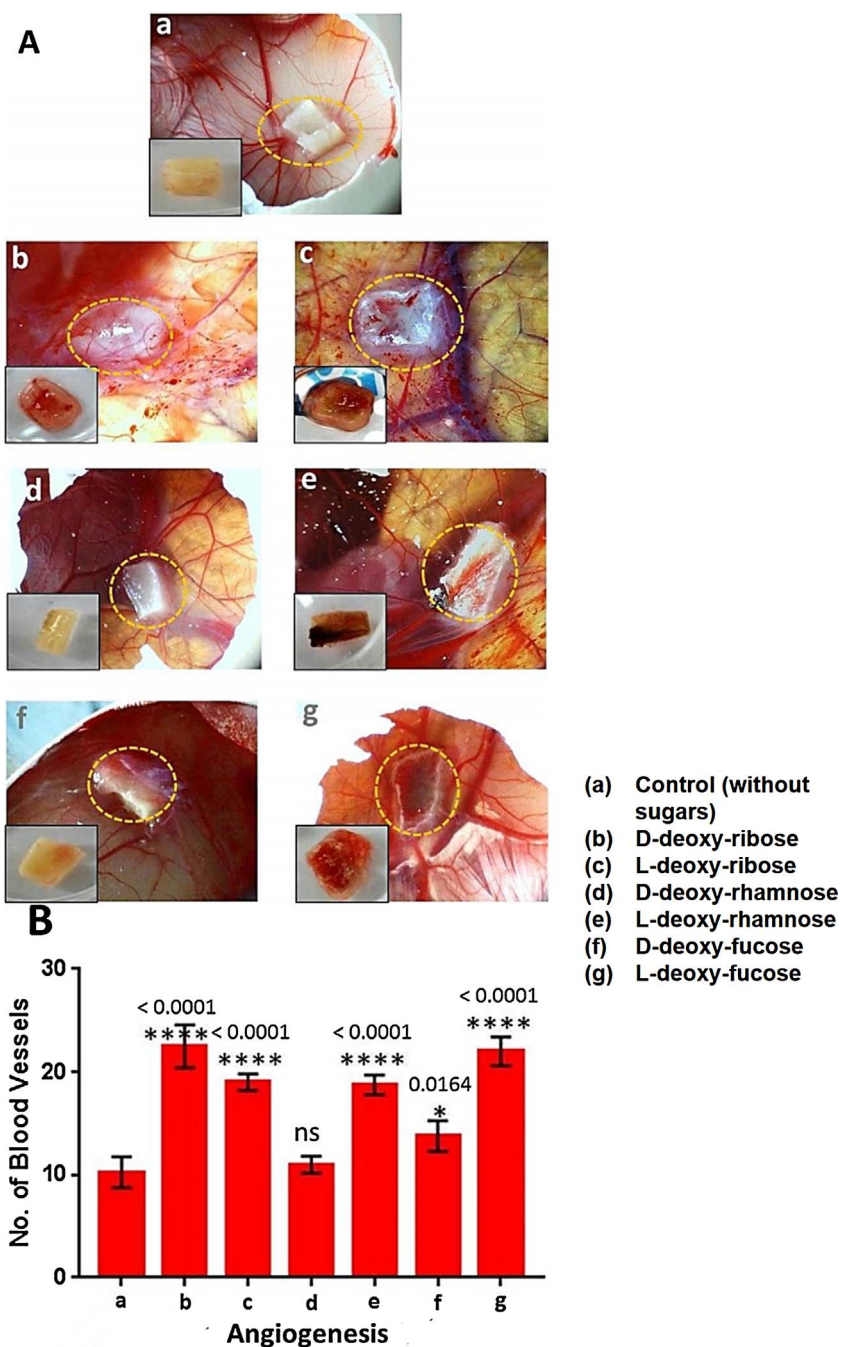


Fig. 4. Proangiogenic potential of CS/Collagen hydrogels using the CAM assay. [A] The hydrogels were placed onto the CAM at day 8 of fertilization. The figure shows light microscope images of hydrogels on CAM at day 14 of fertilization (a) control (without sugars), (b) D-deoxy-ribose loaded hydrogel, (c) L-deoxy-ribose loaded hydrogel, (d) D-deoxy-rhamnose loaded hydrogel, (e) L-deoxy-rhamnose loaded hydrogel, (f) D-deoxy-fucose loaded hydrogel, (g) L-deoxy-fucose loaded hydrogel. The figure also shows respective explanted hydrogels in the lower left corner of each picture. For each experiment 10 eggs were implanted with the respective hydrogels out of which 7 chicks survived. [B] The lower part of the picture shows statistical analysis of the number of blood vessel for each hydrogel. (a) control (without sugars), (b) D-deoxy-ribose loaded hydrogel, (c) L-deoxy-ribose loaded hydrogel, (d) D-deoxy-rhamnose loaded hydrogel, (e) L-deoxy-rhamnose loaded hydrogel, (f) D-deoxy-fucose loaded hydrogel, (g) D-deoxy-fucose loaded hydrogel. Statistical p values are given above the graphical bars. The values shown are means ± S.D. of seven chicks for each hydrogel.

Table 1
The ability of bacteria to ferment sugars.

Bacteria	Deoxy-L-ribose	Deoxy-D-ribose	Deoxy-L-fucose	Deoxy-D-fucose	Deoxy-L-rhamnose	Deoxy-D-rhamnose	Glucose
<i>S. aureus</i>							
S235 ^a	-	-	-	-	-	-	+
NCTC 6571 ^b (Oxford)	-	-	-	-	-	-	+
Newman ^c	-	-	-	-	-	-	+
L-9879 ^d	-	-	-	-	-	-	+
<i>P. aeruginosa</i>	+	+	-	+	-	+	+

^a Clinical strain used previously in infection model.

^b A reference strain used for antibiotic sensitivity testing.

^c Originating from a clinical strain with a defect in surface fibronectin binding protein.

^d A hydrophilic strain.

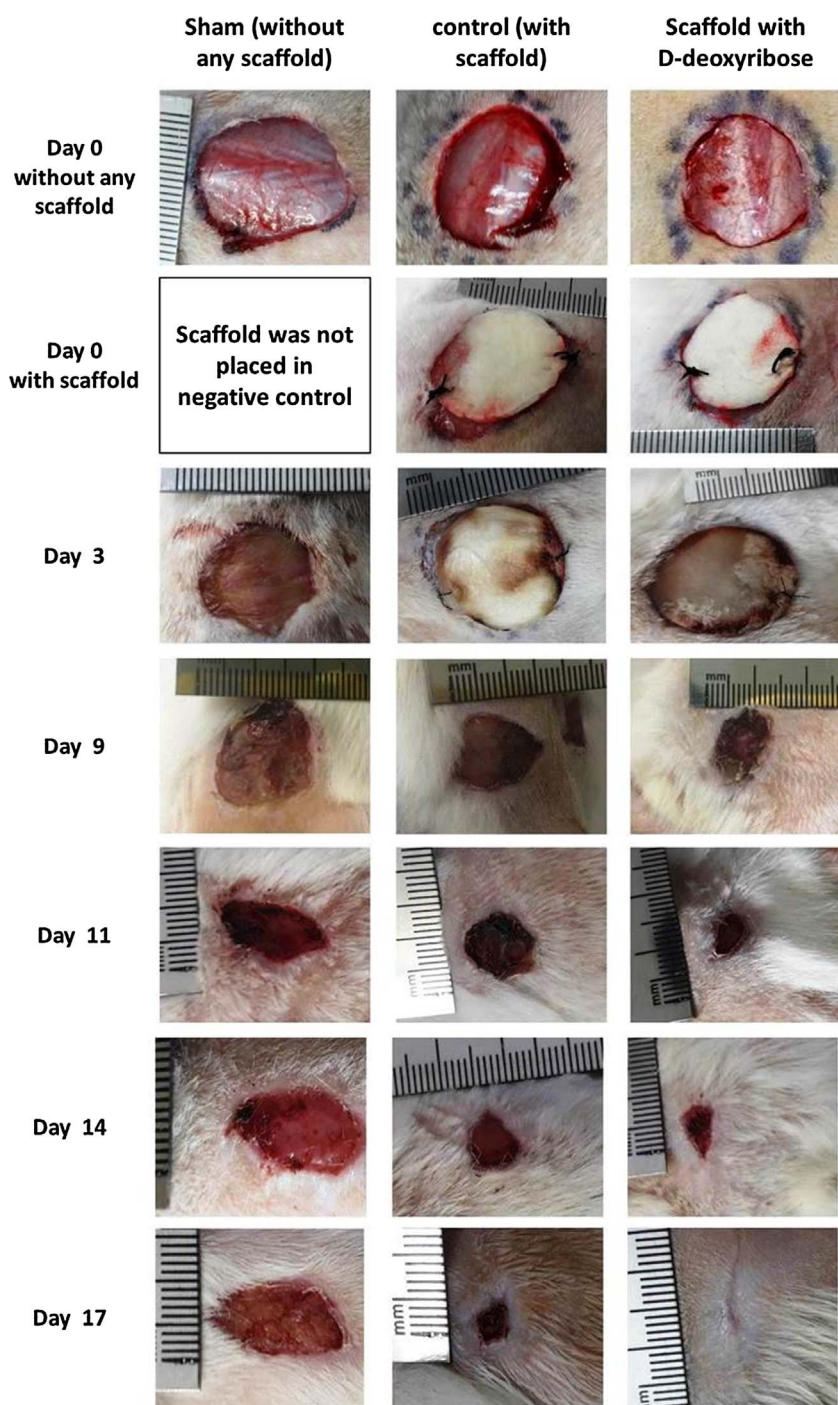


Fig. 5. Representative macroscopic pictures of wounds (sham), control hydrogels (cross-linked CS/collagen hydrogel) and D-ribose loaded hydrogels are shown at days 3, 9, 11, 14 and 17 post-wounding.

robust to handle and indeed could be sutured in place. At day 3, 2-deoxy-D-ribose-loaded hydrogels were very much attached to the surrounding tissues as compared to the other tested materials with an evident ingrowth of cells (Fig. 5), and when stretched manually showed good mechanical strength of the wounds. At day 9, control and D-deoxy-ribose loaded hydrogels were still intact. However, the hydrogels were gradually absorbed and by day 11 more than 50% of the wound area was healed with the deoxy-D-ribose hydrogel (Fig. 6). For those treated with deoxy-D-ribose, by day 11 there was a further decrease in the wound area, by day 14 there was no sign of deoxy-D-sugar hydrogel remaining on the wound, and by day 17 the wound was completely healed in contrast to control wounds and those treated with hydrogels alone (Fig. 5). This hydrogel appeared to be totally absorbed by the animal and could not be felt inside the healed skin when palpating. The

control hydrogel maintained its integrity until the end of the animal study. The remnant control hydrogel was present on the wound till day 17.

Statistical analysis showed that unloaded hydrogels significantly accelerated wound healing and the addition of D-deoxy-ribose greatly accelerated wound healing as can be seen by days 9, 11, 14 and 17 ($p < 0.0001$) (Fig. 6).

3.6. Histological and immunohistochemistry analysis of excised wound tissues

Samples from all groups were harvested on day 17, and were compared to normal skin from a non-treated rat.

At 17 days wound healing in the group treated with 2-deoxy-D-

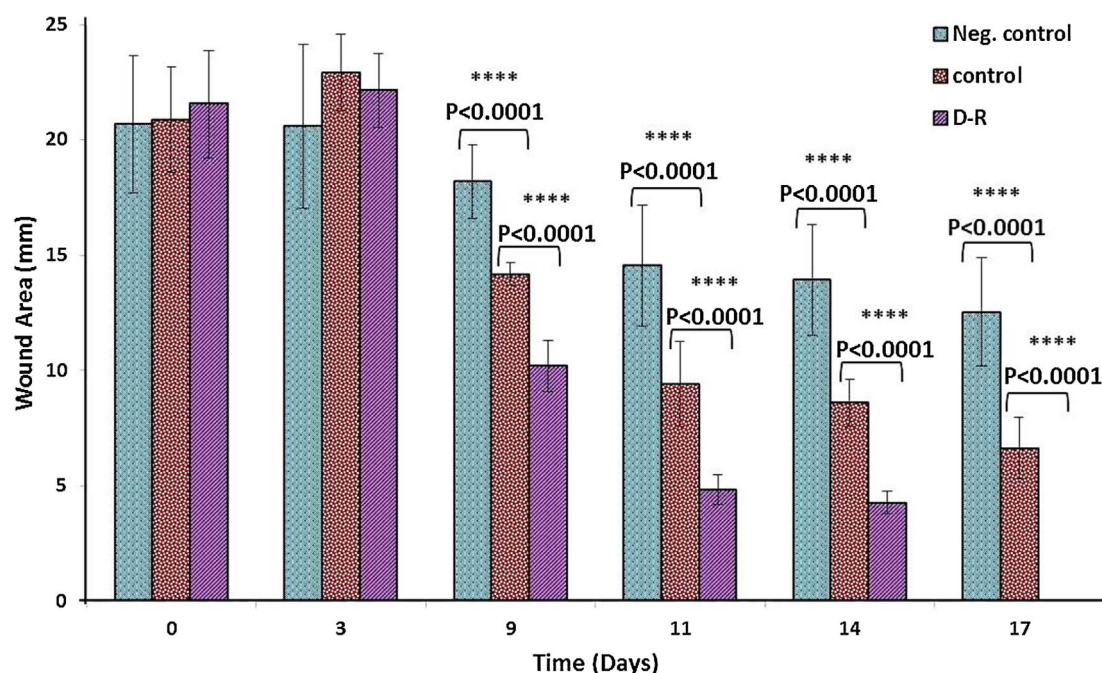


Fig. 6. Wound areas at 0, 3, 9, 11, 14 and 17 days are shown in the histograms. Negative control (open wound left to heal naturally); Control (CS/Collagen hydrogel without sugar); and D-R (CS/Collagen hydrogel loaded with 2-deoxy-D-ribose). Results shown as mean \pm SD, n = 3.

ribose was essentially complete and the structure of the explanted tissue was similar to normal skin as demonstrated by H & E staining (Fig. 7). Gouldern's Trichrome stains in blue/green collagen while muscle, epithelium, hair follicles and blood vessels are stained in red. Apart from the muscle layer stained under the skin as shown for the normal group, the rest looks very similar to the deoxy-D-ribose treated group with an epithelium and hair follicles already formed. In contrast, sham and control groups still showed disorganized granulation wound tissue by 17 days (Fig. 7).

Three different antigens were used for the IHC (CD34 for progenitor endothelial cells, CD80 for M1 macrophages and CD163 for M2 macrophages). CD34 staining demonstrated extensive new blood vessels through the whole thickness of the healed area for the deoxy-D-ribose group. Blind scoring of CD34 staining for this group showed it to be significantly higher than for the control and sham groups also and even higher than in the normal non-wounded group (Fig. 7).

Macrophages expressing M1 response markers are associated with implant rejection and activation of a chronic inflammatory response, while the M2 response markers are expressed by macrophages with an inflammatory response associated with constructive remodelling [33]. As expected, there was no staining for M1 or M2 macrophages for the normal unwounded group (Fig. 7). Some M1 and M2 macrophages were seen in the other groups as would be expected post wounding or post implantation of materials into animals. The table shown in Fig. 7 shows an assessment of the extent of macrophage presence undertaken by blind scoring by research staff in the laboratory. The ratio of M2 to M1 presence was around 1 for wounded animals and those treated with the unloaded CS. For those groups treated with CS loaded with 2-deoxy-D-ribose it was slightly (non-significantly) greater (Fig. 7).

4. Discussion

It is generally believed that biomaterials which help in the rapid growth and infiltration of blood vessels show better biocompatibility than those which exhibit delayed angiogenesis and continued inflammation [34]. Consequently, this is a very desirable property for tissue engineering materials to ensure survival of the tissues.

The aim of this study was to test the hypothesis that the gradual

release of 2-deoxy-D-ribose from biomaterials will promote the production of new blood vessels and hence be of value in wound healing. As previously stated, VEGF is known to be a key mitogen in the induction of new blood vessels but delivered on its own it has proven to be disappointing. Arguably a more productive approach would be to initiate its induction *in vivo* using a biological system that leads to its up-regulation. Looking into literature the current picture concerning the angiogenic activity of the deoxy-sugars is far from clear. Merchan et al. in 2010 reported anti-angiogenic activity of 2-deoxy-D-glucose. They found that this sugar inhibited the angiogenic potential of endothelial cells [35]. In contrast, a paper reported by one of the authors in 2014 [24] that activation of phosphorylase kinase lead to the production of a D-sugar (2-deoxy-D-ribose). This D-sugar in turn led to the production of VEGF in tumourigenesis [24]. Our thinking was to introduce this D-sugar to a biomaterial to see if it could promote angiogenesis. Accordingly, this deoxy-D-sugar was loaded into biodegradable hydrogels of CS/collagen.

The main findings of the study were that this sugar could be readily incorporated into biomaterials and we confirmed that it was indeed proangiogenic using the CAM assay. Also using this assay, we explored to what extent the angiogenic properties of the D isomer of deoxy-ribose were shared with other deoxy-sugars. Here we found that all three L isomers of deoxy-sugars (ribose, fucose and rhamnose) were proangiogenic but only the D isomer of deoxy-ribose was significantly angiogenic.

Looking at the ability of these sugars, to act as metabolic substrates for bacteria, we looked at four strains of *S. aureus* but none of them were able to metabolise these sugars. This is encouraging news in seeking to develop biomaterials containing these sugars as they are not a direct source of nutrients for bacteria. Unfortunately, the Gram negative species, *Pseudomonas aeruginosa*, was able to metabolise all deoxy-sugars except for the L isomers of deoxy-fucose and rhamnose. The reason for investigating the ability of these sugars to act as substrates for bacteria is that if one is preparing a biomaterial to be used on burn wounds or chronic wounds then it would be preferable to use materials that could not be metabolised easily by bacteria.

The next step was to assess the contribution of the D isomer of deoxy-ribose to wound healing *in vivo*. For this we used a rat cutaneous

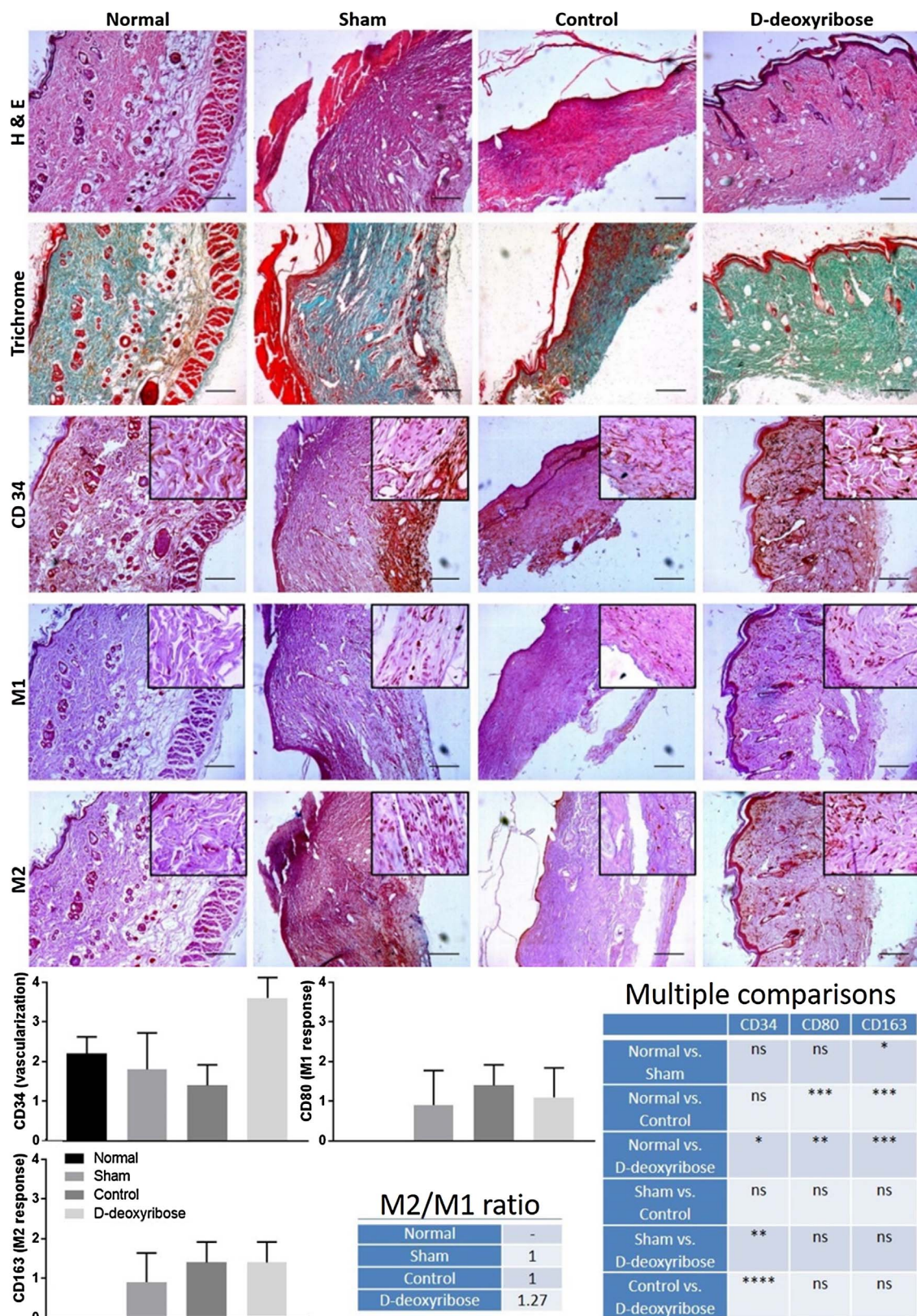


Fig. 7. From top to bottom; H & E, Goldren-trichrome and immunostaining images at day 17. Scale bars of 0.2 mm. Assessment of the immunostaining data using a blind scoring system. 0 = absence; 1 = mild presence; 2 = large presence; 3 = abundance; 4 = great abundance. Results shown are means ± SD, n = 10. Statistics for multiple comparisons and the M2/M1 ratio are shown too.

wound model. The addition of deoxy-D-ribose to a CS/collagen hydrogel greatly accelerated cutaneous wound healing associated with an increase in vascularisation as detected by staining for CD34 positive cells. It was clear from this model that the CS collagen gel itself stimulated wound healing but this was greatly increased by the addition of the D sugar. By day 17 the D sugar treated wounds had completely closed and histology showed the presence of very mature hair follicles. On the basis of this evidence we would conclude that the release of D sugar from a CS/collagen gel stimulates angiogenesis and we propose that the increased wound healing is a natural consequence of this.

Examination of the macrophage response to the deoxy-sugar showed a slight preponderance of M2 macrophages over M1 macrophages by day 17 indicative of constructive remodelling.

We suggest these deoxy-sugar-releasing hydrogels are a promising approach to stimulate angiogenesis in chronic non-healing wounds and also to act as a dermal replacement material in the management of extensive full thickness burns as will be discussed shortly.

If successful there will be several advantages to using this D-sugar to stimulate VEGF production; it is stable and inexpensive and can be introduced into biomaterials to give sustained release over several days to stimulate the growth of new blood vessels. One particular application would be for use on extensive full thickness skin loss due to burns injuries. Here the loss of barrier function can be life-threatening [36,37]. The first-line treatment is always the use of autologous split-skin grafts but in extensively burned patients there are insufficient grafts available to achieve rapid restoration of the barrier layer [38]. Despite 30 years of research in this area there remains a need for a functional and cost-effective permanent dermal substitute to assist surgeons in managing patients with more than 30% full thickness skin loss [36].

When burns extend to more than 30 or 40% of the total body surface area then burns surgeons will seek to use other materials, natural and synthetic, to provide immediate wound cover and aid in the eventual replacement of both the dermis and the epidermis [39]. It remains technically very difficult to produce a tissue engineered material that is equivalent to a split thickness skin graft (containing all of the epidermis and some of the dermis) that will “take” successfully on these wound beds [40]. The major challenge is not in the production of the materials in the laboratory (see Boyce *et al*) [41] but in the tissue engineered materials surviving engraftment on the wound bed, which requires rapid ingrowth of new blood vessels from the underlying wound bed [41,42]. In practice, graft survival is entirely reliant on the growth of new blood vessels from the underlying wound bed into these tissue engineered materials which lack any intrinsic vasculature [43,44].

In practice, full thickness burns are usually treated in two stages (where insufficient autograft is available). Materials are used to provide a vascularised dermal substitute and then when this dermis is well vascularised then either a thin split thickness graft is placed on top of this (often by taking further skin grafts from the initial donor sites once healed) or cultured cells are placed over the vascularised dermis. The two most commonly used materials to provide a vascularised dermis are a biomaterial, Integra, which has been developed for this purpose and donor cadaveric skin [45–47]. Integra is composed of a substrate of bovine collagen with shark chondroitin sulphate onto which a silicon membrane has been bonded [36]. The burn wound is excised clinically, Integra put in place and then left in place until it becomes vascularised which often takes three weeks or more. At this point surgeons can remove the silicon barrier membrane and place on top of it a thin split thickness skin graft. The alternative material that is used is cadaveric skin. This can be used to provide immediate wound cover (once the burned tissue is excised) and restore the barrier function. It then becomes vascularised within the space of a few weeks and the donor epidermis can then be gently removed leaving the donor vascularised dermis in place and the epidermal barrier is replaced with a split thickness skin graft from the patient or with epidermal cells cultured from the patient (as discussed in MacNeil 2007) [48]. However, these materials are not always available to burns surgeons throughout the

world because of the lack of well-run skin banks (for donor skin) or because the purchase of Integra is viewed as too expensive. Consequently, there remains a need for new effective and affordable biomaterials to provide a well vascularised dermal substrate in the management of major burns. The key issue is that none of the current materials contain any intrinsic vasculature hence ingrowth of vessels depends entirely on the blood vessels in the underlying wound bed [42,49]. We suggest that a CS-based hydrogel releasing deoxy-D-ribose merits further exploration as a substitute for a dermis as it will stimulate new blood vessel ingrowth and provide a vascularised wound bed for subsequent grafting with a thin skin graft or cultured autologous keratinocytes to provide a permanent skin barrier layer.

While the current study demonstrates clear functional wound healing properties of a hydrogel loaded with 2 deoxy D ribose there is much more that needs to be understood. It's not clear from this study why one D isomer of a sugar worked and the other 2 did not. This study does not explain the difference between L and D isomers in their mechanism of action. We did not in this study look at the rate of sugar release from the hydrogels. Also, it would have been ideal to conduct wound healing experiments in an animal model with compromised vascularity and wound healing such as a diabetic mouse model. Unfortunately, we were unable to obtain any of these animal models in Pakistan and this will be an important study for the future. Another key question is whether the angiogenic response to the sugar-releasing hydrogel is due to the up-regulation of VEGF – we did not seek to examine that in this study – assessing the VEGF release and blocking the action of the VEGF to see if that negates the response to the sugar-releasing hydrogel will also help elucidate the mechanism of action at least to the point of confirming whether the angiogenesis is dependent on a regulation of the VEGF or not.

Thus, now that we have confirmed the potent wound healing response to the 2-deoxy-D ribose sugar further studies are merited to obtain information on the mechanism of action and indeed to compare its potency to the addition of the VEGF on its own.

5. Conclusion

We conclude that as the delivery of 2-deoxy-D-ribose from a hydrogel stimulates angiogenesis in both the CAM assay and a rat wound healing model this offers an important new approach to developing pro-angiogenic wound healing materials for clinical use which merits further development.

Acknowledgements

We gratefully acknowledge support from COMSATS University, Pakistan for a Pakistan/UK Fellowship for Dr M. Yar to work with Prof MacNeil. We are grateful to the University of Sheffield IIR fund for support of Dr Roman.

References

- [1] Q. Zhang, J. Hubenak, T. Iyyanki, E. Alred, K.C. Turza, G. Davis, E.I. Chang, C.D. Branch-Brooks, E.K. Beahm, C.E. Butler, Engineering vascularized soft tissue flaps in an animal model using human adipose-derived stem cells and VEGF + PLGA/PEG microspheres on a collagen-chitosan scaffold with a flow-through vascular pedicle, *Biomaterials* 73 (2015) 198–213.
- [2] Y. Miyagi, L.L. Chiu, M. Cimini, R.D. Weisel, M. Radisic, R.-K. Li, Biodegradable collagen patch with covalently immobilized VEGF for myocardial repair, *Biomaterials* 32 (5) (2011) 1280–1290.
- [3] A. Khojasteh, F. Fahimipour, M.B. Eslaminejad, M. Jafarian, S. Jahangir, F. Bastami, M. Tahriri, A. Karkhaneh, L. Tayebi, Development of PLGA-coated β -TCP scaffolds containing VEGF for bone tissue engineering, *Mat. Sci. Eng. C* 69 (2016) 780–788.
- [4] K.E. Johnson, T.A. Wilgus, Vascular endothelial growth factor and angiogenesis in the regulation of cutaneous wound repair, *Adv. Wound Care* 3 (10) (2014) 647–661.
- [5] B.L. Long, R. Rekhi, A. Abrego, J. Jung, A.A. Qutub, Cells as state machines: cell behavior patterns arise during capillary formation as a function of BDNF and VEGF, *J. Theor. Biol.* 326 (2013) 43–57.
- [6] H. Xin, C. Zhong, E. Nudleman, N. Ferrara, Evidence for pro-angiogenic functions of

- VEGF-Ax, *Cell* 167 (1) (2016) 275–284. e6..
- [7] M. Simons, E. Gordon, L. Claesson-Welsh, Mechanisms and regulation of endothelial VEGF receptor signalling, *Nat. Rev. Mol. Cell Biol.* 17 (10) (2016) 611–625.
- [8] L.L. Chiu, M. Radisic, Scaffolds with covalently immobilized VEGF and Angiopoietin-1 for vascularization of engineered tissues, *Biomaterials* 31 (2) (2010) 226–241.
- [9] N. Çakır-Özkan, S. Eğri, E. Bekar, B.Z. Altunkaynak, Y.B. Kabak, E.G. Kıvrak, The use of sequential VEGF-and BMP2-Releasing biodegradable scaffolds in rabbit mandibular defects, *J. Oral Maxillofac. Surg.* 75 (1) (2017) 221. e1-221. e14..
- [10] Y. Zhang, J. Huang, L. Huang, Q. Liu, H. Shao, X. Hu, L. Song, Silk fibroin-based scaffolds with controlled delivery order of VEGF and BDNF for cavernous nerve regeneration, *ACS Biomater. Sci. Eng.* 2 (11) (2016) 2018–2025.
- [11] L. Zhao, S. Ma, Y. Pan, Q. Zhang, K. Wang, D. Song, X. Wang, G. Feng, R. Liu, H. Xu, Functional modification of fibrous PCL scaffolds with fusion protein VEGF-HGFI enhanced cellularization and vascularization, *Adv. Healthc. Mater.* 5 (18) (2016) 2376–2385.
- [12] J. Wu, J. Ye, J. Zhu, Z. Xiao, C. He, H. Shi, Y. Wang, C. Lin, H. Zhang, Y. Zhao, Heparin-based coacervate of FGF2 improves dermal regeneration by asserting a synergistic role with cell proliferation and endogenous facilitated VEGF for cutaneous wound healing, *Biomacromolecules* 17 (6) (2016) 2168–2177.
- [13] G. Gigliobianco, C.K. Chong, S. MacNeil, Simple surface coating of electrospun poly-L-lactic acid scaffolds to induce angiogenesis, *J. Biomater. Appl.* 30 (1) (2015) 50–60.
- [14] L. Gilmore, S. Rimmer, S.L. McArthur, S. Mittar, D. Sun, S. MacNeil, Arginine functionalization of hydrogels for heparin binding—a supramolecular approach to developing a pro-angiogenic biomaterial, *Biotechnol. Bioeng.* 110 (1) (2013) 296–317.
- [15] C. Easton, A. Bullock, G. Gigliobianco, S. McArthur, S. MacNeil, Application of layer-by-layer coatings to tissue scaffolds—development of an angiogenic biomaterial, *J. Mater. Chem. B* 2 (34) (2014) 5558–5568.
- [16] N. Ferrara, H.-P. Gerber, J. LeCouter, The biology of VEGF and its receptors, *Nat. Med.* 9 (6) (2003) 669–676.
- [17] J.H. Harmey, VEGF and Cancer, Springer Science & Business Media, 2004.
- [18] D.J. Hicklin, L.M. Ellis, Role of the vascular endothelial growth factor pathway in tumor growth and angiogenesis, *J. Clin. Oncol.* 23 (5) (2005) 1011–1027.
- [19] Q. Tan, B. Chen, X. Yan, Y. Lin, Z. Xiao, X. Hou, J. Dai, Promotion of diabetic wound healing by collagen scaffold with collagen-binding vascular endothelial growth factor in a diabetic rat model, *J. Tissue Eng. Regen. Med.* 8 (3) (2014) 195–201.
- [20] Z. Xie, C.B. Paras, H. Weng, P. Punnakitikashem, L.-C. Su, K. Vu, L. Tang, J. Yang, K.T. Nguyen, Dual growth factor releasing multi-functional nanofibers for wound healing, *Acta Biomater.* 9 (12) (2013) 9351–9359.
- [21] R. Guo, S. Xu, L. Ma, A. Huang, C. Gao, The healing of full-thickness burns treated by using plasmid DNA encoding VEGF-165 activated collagen?chitosan dermal equivalents, *Biomaterials* 32 (4) (2011) 1019–1031.
- [22] T. Simón-Yarza, F.R. Formiga, E. Tamayo, B. Pelacho, F. Prosper, M.J. Blanco-Prieto, Vascular endothelial growth factor-delivery systems for cardiac repair: an overview, *Theranostics* 2 (6) (2012) 541–552.
- [23] M. Thompson, Oxford Textbook of Vascular Surgery, Oxford University Press, 2016.
- [24] S.A. Shahzad, M. Yar, M. Bajda, B. Jadoon, Z.A. Khan, S.A.R. Naqvi, A.J. Shaikh, K. Hayat, A. Mahmood, N. Mahmood, S. Filipek, Synthesis and biological evaluation of novel oxadiazole derivatives: a new class of thymidine phosphorylase inhibitors as potential anti-tumor agents, *Biorg. Med. Chem.* 22 (3) (2014) 1008–1015.
- [25] M. Christensen, T. Borza, G. Dandanell, A.-M. Gilles, O. Barzu, R.A. Kelln, J. Neuhard, Regulation of expression of the 2-deoxy-D-ribose utilization regulon, *deoQKPX*, from *Salmonella enterica* serovar typhimurium, *J. Bacteriol.* 185 (20) (2003) 6042–6050.
- [26] M. Farooq, A.S. Yar, L. Khan, S.A. Shahzadi, N. Siddiqi, A. Mahmood, F. Rauf, A.A. Chaudhry, I. ur Rehman, Synthesis of piroxicam loaded novel electrospun biodegradable nanocomposite scaffolds for periodontal regeneration, *Mat. Sci. Eng. C* 56 (2015) 104–113.
- [27] J. Shepherd, I. Douglas, S. Rimmer, L. Swanson, S. MacNeil, Development of three-dimensional tissue-engineered models of bacterial infected human skin wounds, *Tissue Eng. Part C Methods* 15 (3) (2009) 475–484.
- [28] M. Yar, G. Gigliobianco, L. Shahzadi, L. Dew, S.A. Siddiqi, A.F. Khan, A.A. Chaudhry, I. u. Rehman, S. MacNeil, Production of chitosan PVA PCL hydrogels to bind heparin and induce angiogenesis, *Int. J. Polym. Mater.* 65 (9) (2016) 466–476.
- [29] A. Islam, T. Yasin, Controlled delivery of drug from pH sensitive chitosan/poly (vinyl alcohol) blend, *Carbohydr. Polym.* 88 (3) (2012) 1055–1060.
- [30] M. Tehi, J. Sheikh, Extraction of chitosan from shrimp shells waste and application in antibacterial finishing of bamboo rayon, *Int. J. Biol. Macromol.* 50 (5) (2012) 1195–1200.
- [31] A.P. Rokhade, S.A. Patil, T.M. Aminabhavi, Synthesis and characterization of semi-interpenetrating polymer network microspheres of acrylamide grafted dextran and chitosan for controlled release of acyclovir, *Carbohydr. Polym.* 67 (4) (2007) 605–613.
- [32] S. Yar, S.A. Shahzad, N. Siddiqi, A. Mahmood, M.S. Rauf, A.A. Chaudhry, I. ur Rehman, Triethyl orthoformate mediated a novel crosslinking method for the preparation of hydrogels for tissue engineering applications: characterization and in vitro cytocompatibility analysis, *Mat. Sci. Eng. C* 56 (2015) 154–164.
- [33] S.F. Badyal, J.E. Valentin, A.K. Ravindra, G.P. McCabe, A.M. Stewart-Akers, Macrophage phenotype as a determinant of biologic scaffold remodeling, *Tissue Eng. Pt. A* 14 (11) (2008) 1835–1842.
- [34] M.T. Wolf, C.L. Dearth, C.A. Ranallo, S.T. LoPresti, L.E. Carey, K.A. Daly, B.N. Brown, S.F. Badyal, Macrophage polarization in response to ECM coated polypropylene mesh, *Biomaterials* 35 (25) (2014) 6838–6849.
- [35] J.R. Merchan, K. Kovacs, J.W. Railsback, M. Kurtoglu, Y. Jing, Y. Pina, N. Gao, T.G. Murray, M.A. Lehrman, T.J. Lampidis, Antiangiogenic activity of 2-deoxy-D-glucose, *PLoS One* 5 (10) (2010) e13699.
- [36] A.W.C. Chua, Y.C. Khoo, B.K. Tan, K.C. Tan, C.L. Foo, S.J. Chong, Skin tissue engineering advances in severe burns: review and therapeutic applications, *Burns Trauma* 4 (1) (2016) 3.
- [37] M. Blais, R. Parenteau-Bareil, S. Cadau, F. Berthod, Concise review: tissue-engineered skin and nerve regeneration in burn treatment, *Stem Cell Transl. Med.* 2 (7) (2013) 545–551.
- [38] J.W. Yi, J.K. Kim, Prospective randomized comparison of scar appearances between cograf of acellular dermal matrix with autologous split-thickness skin and autologous split-thickness skin graft alone for full-thickness skin defects of the extremities, *Plast. Reconstr. Surg.* 135 (3) (2015) 609e–616e.
- [39] K. Sharma, A. Bullock, D. Ralston, S. MacNeil, Development of a one-step approach for the reconstruction of full thickness skin defects using minced split thickness skin grafts and biodegradable synthetic scaffolds as a dermal substitute, *Burns* 40 (5) (2014) 957–965.
- [40] S. Böttcher-Haberzeth, T. Biedermann, E. Reichmann, Tissue engineering of skin, *Burns* 36 (4) (2010) 450–460.
- [41] S.T. Boyce, R.J. Kagan, K.P. Yakuboff, N.A. Meyer, M.T. Rieman, D.G. Greenhalgh, G.D. Warden, Cultured skin substitutes reduce donor skin harvesting for closure of excised, full-thickness burns, *Ann. Surg.* 235 (2) (2002) 269–279.
- [42] D.M. Supp, S.T. Boyce, Engineered skin substitutes: practices and potentials, *Clin. Dermatol.* 23 (4) (2005) 403–412.
- [43] M.W. Laschke, Y. Harder, M. Amon, I. Martin, J. Farhadi, A. Ring, N. Torio-Padron, R. Schramm, M. Rücker, D. Junker, Angiogenesis in tissue engineering: breathing life into constructed tissue substitutes, *Tissue Eng.* 12 (8) (2006) 2093–2104.
- [44] S. Hacker, R. Mittermayr, S. Nickl, T. Haider, D. Leberz-Eichinger, L. Beer, A. Mitterbauer, H. Leiss, M. Zimmermann, T. Schweiger, Paracrine factors from irradiated peripheral blood mononuclear cells improve skin regeneration and angiogenesis in a porcine burn model, *Sci. Rep.* 6 (2016).
- [45] D.Q. Nguyen, T.S. Potokar, P. Price, An objective long-term evaluation of Integra (a dermal skin substitute) and split thickness skin grafts, in acute burns and reconstructive surgery, *Burns* 36 (1) (2010) 23–28.
- [46] R. Weigert, H. Choughri, V. Casoli, Management of severe hand wounds with Integra® dermal regeneration template, *J. Hand Surg. Eur.* 36 (3) (2011) 185–193.
- [47] H. Cleland, J. Wasiaak, H. Dobson, M. Paul, G. Pratt, E. Paul, M. Herson, S. Akbarzadeh, Clinical application and viability of cryopreserved cadaveric skin allografts in severe burn: a retrospective analysis, *Burns* 40 (1) (2014) 61–66.
- [48] S. MacNeil, Progress and opportunities for tissue-engineered skin, *Nature* 445 (7130) (2007) 874–880.
- [49] P.S. Sahota, J.L. Burn, M. Heaton, E. Freedlander, S.K. Suvarna, N.J. Brown, S. Mac Neil, Development of a reconstructed human skin model for angiogenesis, *Wound Repair Regen.* 11 (4) (2003) 275–284.